Journal of the European Ceramic Society xxx (xxxx) xxx–xxx

Contents lists available at ScienceDirect

Journal of the European Ceramic Society

journal homepage: www.elsevier.com/locate/jeurceramsoc

Original Article

# A novel temperature-stable $Ba_{2-x}Ca_xMgTi_5O_{13}$ microwave dielectric ceramic

Qianlong Dai[a], Ruzhong Zuo[a,*], Yudong Xu[a], Liangguo He[b]

[a] Institute of Electro Ceramics & Devices, School of Materials Science and Engineering, Hefei University of Technology, Hefei, 230009, PR China
[b] School of Mechanical Engineering, Hefei University of Technology, Hefei, 230009, PR China

ARTICLE INFO

*Keywords:*
Microwave dielectric ceramics
Bond valence
Sintering
Packing fraction

ABSTRACT

The $Ba_{2-x}Ca_xMgTi_5O_{13}$ ($0 \le x \le 0.3$) microwave dielectric ceramics were for the first time prepared via a conventional solid-state reaction method. A small amount of $Ca^{2+}$ can dissolve into the lattice by forming solid solutions with a monoclinic structure (C2/m) and further influence the sintering behavior, grain growth and microwave dielectric properties of $Ba_{2-x}Ca_xMgTi_5O_{13}$ ceramics. Both increase of $\varepsilon_r$ and decrease of Qxf with x should be associated with increased lattice distortion and uneven grain growth although the sample density and the ratio of the ionic polarizability to the molar volume show little variation. Moreover, the A-site bond valence and $\tau_f$ indicate a close relation in current study, such that the $Ca^{2+}$ substitution can induce an increase of $\tau_f$ values. The optimum microwave dielectric properties of $\varepsilon_r \sim 29.3$, Qxf ~ 30,870 GHz (6.5 GHz), and a near-zero $\tau_f \sim +2.1$ ppm/°C can be contained in the x = 0.15 ceramic sintered at 1160 °C.

## 1. Introduction

Microwave dielectric ceramics have been widely used for the fabrication of filters, dielectric antennas, dielectric resonator and dielectric substrates in the field of wireless communications, such as mobile phone, wireless local area networks and global position systems [1–3], In recent years, millimeter waves for wireless communications such as 5 G technology have been well known as a hot spot in research area. Microwave dielectric ceramics are usually expected to have a high dielectric constant ($\varepsilon_r$) for devices miniaturization, a high quality factor (Qxf) to achieve excellent cross-coupling selectively, and a near-zero temperature coefficient of resonant frequency ($\tau_f$) to ensure the stability of transmitted frequency, although $\varepsilon_r$ is expected to be as small as possible for millimeter-wave wireless communication.

Up to now, compounds such as $BaTi_4O_9$ and $Ba_2Ti_9O_{20}$ based on the BaO-$TiO_2$ system with superior microwave dielectric properties have been extensively investigated and widely used in producing various microwave devices such as resonators, filters, oscillators and so on [4,5]. In order to improve their microwave dielectric properties, appropriate amount of ZnO, $Al_2O_3$, $Nb_2O_5$ and $Ln_2O_3$ (Ln = La, Sm, Nd, etc.) were added to the BaO-$TiO_2$ system during the raw material stage [6–12]. The BaO-ZnO-$TiO_2$ system has been found to contain four ternary phases such as $Ba_4ZnTi_{11}O_{27}$, $BaZn_2Ti_4O_{11}$, $Ba_2ZnTi_5O_{13}$ and hollandite-type solid solutions $Ba_xZn_xTi_{8-x}O_{16}$ [13]. The BaO-$Ln_2O_3$-$TiO_2$ system was reported to contain either $BaLn_2Ti_5O_{14}$ or $BaLn_2Ti_4O_{12}$ as its major phase. All these compounds have exhibited good microwave dielectric properties, showing potential application values in microwave devices [14,15]. The BaO-MgO-$TiO_2$ ternary system was reported to contain one nonstoichiometric hollandite phase $Ba_xMg_xTi_{8-x}O_{16}$ and three other phases $BaMg_6Ti_6O_{19}$, $Ba_4MgTi_{11}O_{27}$ and $Ba_2MgTi_5O_{13}$, among which microwave dielectric properties of $BaMg_6Ti_6O_{19}$ and $Ba_4MgTi_{11}O_{27}$ ceramics were reported [13,16]. The monoclinic $Ba_2MgTi_5O_{13}$ ceramic has not yet been systematically studied, particularly its microwave dielectric properties. In this paper, $Ba_{2-x}Ca_xMgTi_5O_{13}$ ($0 \le x \le 0.3$) ceramics were prepared by a conventional solid-state reaction method. The effect of the substitution of a small amount of $Ca^{2+}$ for $Ba^{2+}$ on the sintering behavior, phase composition, microstructure and microwave dielectric properties of the ceramics was investigated in detail.

## 2. Experimental

A conventional solid-state reaction method was employed to prepare $Ba_{2-x}Ca_xMgTi_5O_{13}$ ($0 \le x \le 0.3$) ceramics by using high-purity starting powders of analytic-grade $CaCO_3$, $BaCO_3$, MgO and $TiO_2$. The MgO powder was pretreated at 800 °C in air for 2 h to remove any hydroxides before weighing. The raw powders in stoichiometric proportion were weighed and then ball milled using zirconia balls in ethanol medium for 4 h. The resultant slurries were then rapidly dried and calcined at 1100 °C for 6 h in air, followed by a milling process for 6 h. The granulated powders 0.5 wt% PVB were subsequently pressed into cylinders with dimensions of 10 mm in diameter and 7–8 mm in

* Corresponding author.
*E-mail address:* rzzuo@hotmail.com (R. Zuo).

https://doi.org/10.1016/j.jeurceramsoc.2019.09.043
Received 26 July 2019; Received in revised form 24 September 2019; Accepted 24 September 2019

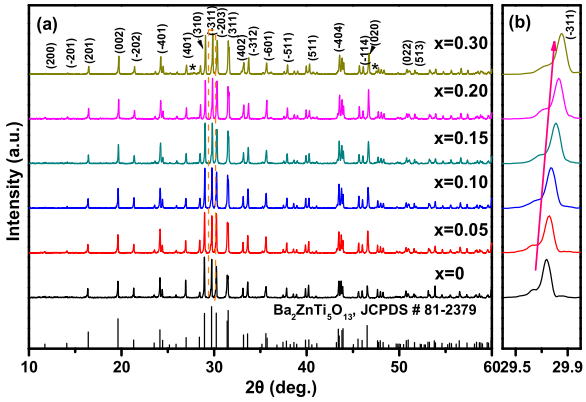


**Fig. 1.** (a) XRD patterns of $Ba_{2-x}Ca_xMgTi_5O_{13}$ ceramics sintered at optimum temperatures for 4 h and (b) locally magnified diffraction peaks near 30°.

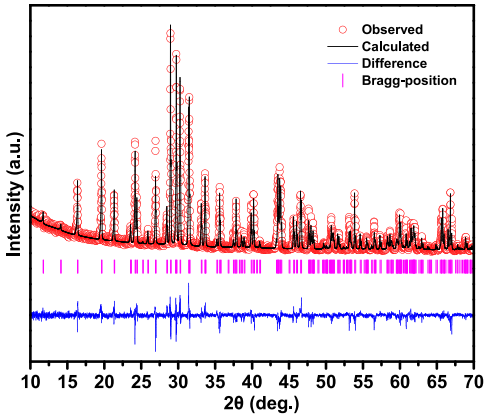


**Fig. 2.** Rietveld refinement plot of the $Ba_{1.85}Ca_{0.15}MgTi_5O_{13}$ ceramic sintered at 1160 °C for 4 h.

height. The specimens were first heated at 550 °C in air for 4 h to remove the organic binder, and then sintered at 1100–1240 °C for 4 h.

The Archimedes method was used to evaluate the bulk densities of the sintered samples. A conventional X-ray diffractometer (XRD; D/Max2500 V, Rigaku, Japan) was employed to collect the diffraction patterns over a 2θ range of 10-70° with a step of 0.02°. The structural parameters were obtained from the Rietveld refinement of XRD data using the GSAS-EXPGUI program. The grain morphology of the sintered samples was observed on polished and thermally etched surfaces using a field-emission scanning electron microscope (FE-SEM; SU8020, JEOL, Tokoy, Japan). A network analyzer (Agilent, N5230C, Palo Alto, CA) was used to measure the $\varepsilon_r$ and unloaded $Q\times f$ value of the well-polished ceramic samples in the $TE_{011}$ mode by means of a Hakki-Coleman post resonator method. The $\tau_f$ values of the samples were measured in the temperature range of 20 ~ 80 °C.

## 3. Results and discussion

Fig. 1(a) shows the normalized XRD pattern of $Ba_{2-x}Ca_xMgTi_5O_{13}$ ($0 \le x \le 0.3$) ceramics sintered at optimum temperatures for 4 h. It is clear that the diffraction peaks of all studied samples can be well assigned to a monoclinic structure with a space group of C2/m (JCPDS No. 81-2379). It should be noted that the main diffraction peaks slightly shift to higher angles with increasing x. as plotted in Fig. 1(b), meaning that the cell volume decreases with increasing $Ca^{2+}$ content. In addition, a small amount of unknown impurity phases start to appear as the substitution content of $Ca^{2+}$ is larger than 0.3. In order to clarify the effect of $Ca^{2+}$ substitution for $Ba^{2+}$ on the crystal structure of $Ba_{2-x}Ca_xMgTi_5O_{13}$ in more detail, the Rietveld refinement was performed by adopting the GSAS-EXPGUI program, in which a structural model of $Ba_2ZnTi_5O_{13}$ was used. The refined plot of the x = 0.15 sample sintered at 1160 °C was selected as an example, as shown in Fig. 2. The lattice parameters, cell volume and reliability factors of $R_{wp}$, $R_P$, and $\chi^2$ for all studied samples are listed in Table 1. $R_{wp}$, $R_P$, and $\chi^2$ values are located in the range of < 10%, < 9%, and 1.7–2.0, respectively, suggesting a valid structural model and a desirable refinement process. It is obvious that the substitution of $Ca^{2+}$ for $Ba^{2+}$ induces a monotonous decrease of the unit cell volume of the studied ceramics owing to the occupation of $Ca^{2+}$ (1.12 Å, CN = 8) with a smaller ionic radius than $Ba^{2+}$ (1.42 Å, CN = 8).

Fig. 3 shows SEM images on polished and thermally etched surfaces of $Ba_{2-x}Ca_xMgTi_5O_{13}$ ($0 \le x \le 0.3$) ceramics sintered at optimum temperatures for 4 h. Compared with the x = 0 sample, the grain size and morphology of $Ba_{2-x}Ca_xMgTi_5O_{13}$ ceramics change significantly with increasing x. The average grain size of the samples gradually increases with increasing x values. Moreover, the grain morphology also ranges from uniformly distributed polygonal grains to larger rod-like grains, although all samples can be well densified at optimum sintering temperatures. The results indicate that the substitution of $Ca^{2+}$ for $Ba^{2+}$ promotes the grain growth and alters the grain morphology to some extents, which might have an effect on the microwave dielectric properties.

Fig. 4 (a–c) shows the variation of relative density and microwave dielectric properties of $Ba_{2-x}Ca_xMgTi_5O_{13}$ ceramics as a function of sintering temperature. As shown in Fig. 4(a), with increasing sintering temperature, the relative densities of all studied samples firstly increase to their respective maximum values at their optimum sintering temperatures, and then decrease with further increasing sintering temperature. This means that all samples exhibit a typical densification behavior and reach high relative densities (> 96%) at the optimum temperature, keeping a good consistency with the microstructure observation. Moreover, the optimum sintering temperature of each composition is slightly reduced with increasing x up to x = 0.1 and then increased thereafter. However, the sample density at its optimum sintering temperature slightly increases at x = 0.05-0.1 and then deceases thereafter, but is larger than 96% for all compositions. On the one hand, $\varepsilon_r$ and Qxf values of $Ba_{2-x}Ca_xMgTi_5O_{13}$ ceramics with increasing sintering temperature present a similar variation tendency with density, as can be seen from Fig. 4(b,c). On the other hand, $\varepsilon_r$ shows a monotonous increase with increasing the substitution content of $Ca^{2+}$ (Fig. 4(d)), but Qxf values of $Ba_{2-x}Ca_xMgTi_5O_{13}$ ceramics show a maximum value at x = 0.05 and then rapidly decreases. Compared with the sample density, $\varepsilon_r$ exhibits a different variation tendency with x. However, the sample density should not have an obvious effect on the $\varepsilon_r$ value, considering all samples have been well densified as mentioned above.

It is well known that $\varepsilon_r$ can be mainly influenced by the dielectric polarizabilities and structural characteristics, as described by the Clausius-Mosotti equation [17]:

$$\varepsilon_r = \frac{3}{1 - b\alpha_D/V_m} - 2 \quad (1)$$

where b is defined as $4\pi/3$, $\alpha_D$ is the ionic polarizability, and $V_m$ is the molecular volume. The polarizability of the unit cell should be altered after the $Ca^{2+}$ substitution, considering that $Ca^{2+}$ (3.16 $Å^3$) has a smaller ionic polarizability than $Ba^{2+}$ (6.40 $Å^3$). According to the Shannon additive rule:

$$\alpha_{theo}(Ba_{2-x}Ca_xMgTi_5O_{13}) = (2-x)\alpha(Ba^{2+}) + (x)\alpha(Ca^{2+}) + \alpha(Mg^{2+}) + 5\alpha(Ti^{4+}) + 13\alpha(O^{2-}) \quad (2)$$

where $\alpha_{theo}$ is the theoretical polarizability, and α(i) (i = $Ba^{2+}$, $Ca^{2+}$, $Mg^{2+}$, $Ti^{4+}$, $O^{2-}$) is the polarizability of constituent ions [18]. As shown in Fig. 4(d), the ratio of the theoretical ionic polarizability to the molar volume ($\alpha_D/V_m$) for the studied compounds was found to slightly decrease from 0.2023 at x = 0 to 0.2015 at x = 0.2, corresponding to a little variation of theoretically predicted permittivity $\varepsilon_{theo}$ from 17.65 at

**Table 1**
Refined structural parameters, bond valence parameter, cation bond valence, reliability factors and goodness-of-fit indicator for $Ba_{2-x}Ca_xMgTi_5O_{13}$ ceramics sintered at optimum sintering temperatures.

| | x = 0.0 | x = 0.05 | x = 0.10 | x = 0.15 | x = 0.20 | x = 0.30 |
|---|---|---|---|---|---|---|
| a (Å) | 15.2421(2) | 15.2389(4) | 15.2345(3) | 15.2253(3) | 15.2189(5) | 15.2124(3) |
| b (Å) | 3.8967(5) | 3.8928(9) | 3.8893(7) | 3.8846(8) | 3.8794(1) | 3.8731(7) |
| c (Å) | 9.1363(8) | 9.1334(1) | 9.1302(1) | 9.1245(1) | 9.1213(1) | 9.1179(1) |
| $V_m$ (Å$^3$) | 542.64(2) | 541.83(2) | 540.98(1) | 539.66(2) | 538.52(2) | 537.21(2) |
| Wyckoff | 4i | 4i | 4i | 4i | 4i | 4i |
| $R_{A\text{-}O}$ | 2.29 | 2.2819 | 2.2739 | 2.2658 | 2.2577 | 2.2416 |
| 2-d(A-O1) | 2.834 | 2.831 | 2.823 | 2.815 | 2.803 | 2.783 |
| 2-d(A-O2) | 2.712 | 2.702 | 2.695 | 2.687 | 2.684 | 2.671 |
| 2-d(A-O3) | 3.059 | 3.051 | 3.047 | 3.040 | 3.032 | 3.016 |
| 2-d(A-O4) | 2.856 | 2.841 | 2.821 | 2.799 | 2.774 | 2.742 |
| $V_{A\text{-}O}$ | 1.782 | 1.788 | 1.798 | 1.814 | 1.832 | 1.853 |
| $R_{wp}$ (%) | 8.55 | 8.57 | 9.10 | 8.95 | 9.11 | 9.08 |
| $R_p$ (%) | 7.27 | 7.98 | 7.22 | 6.55 | 7.42 | 7.42 |
| $\chi^2$ | 1.72 | 1.88 | 1.74 | 1.85 | 1.79 | 1.95 |

$R_{wp}$: the reliability factor of weighted patterns; $R_p$: the reliability factor of patterns; $\chi^2$: goodness-of-fit indicator = $(R_{wp}/R_{exp})^2$.

x = 0 to 17.24 at x = 0.2, which is still unable to explain the variation of the experimental $\varepsilon_r$ with x. Therefore, the change in structural characteristics, such as the distortion, tilting, and rattling spaces of oxygen octahedron in the unit cell, caused by $Ca^{2+}$ substitution may be responsible for the difference between calculated $\varepsilon_{theo}$ and measured $\varepsilon_r$. In addition, the increased relative density after the substitution of a small amount of $Ca^{2+}$ (x < 0.2) (Fig. 4(a)) would help increase $\varepsilon_r$. As x ≥ 0.2, the appearance of unknown secondary phases (Fig. 1) probably with larger $\varepsilon_r$ leads to a further increased $\varepsilon_r$ of the system, although the relative density slightly decreases at this time.

In general, the dielectric loss can be divided into extrinsic loss and intrinsic loss [19]. The extrinsic loss is mainly caused by density, secondary phase, grain size and lattice defects, while the intrinsic loss is mainly caused by structure characteristics. In current work, the $Ba_{2-x}Ca_xMgTi_5O_{13}$ compound remains a single-phase structure as x < 0.3. All studied samples possess high densities (> 96%) at optimum sintering temperatures, so the effect of extrinsic factors could be neglected. Therefore, the structure characteristics should be the dominant factors that influence Qxf values, as evaluated by the packing fraction (f) defined by the summation of the volume of packed ions over the volume of a primitive unit cell. The calculated packing fraction of $Ba_{2-x}Ca_xMgTi_5O_{13}$ ceramics is also presented in Fig. 4(d). The variation of Qxf as a function of sintering temperature is generally consistent with that of packing fraction, meaning the close dependence of Qxf value on packing fraction. An increase in Qxf values at x = 0.05 may be attributed to changes in microstructure including grain size and morphology as mentioned above. Moreover, a small amount of secondary phases at x = 0.30 should also attribute to the rapid deterioration of Qxf values.

Furthermore, Fig. 5 indicates that the $\tau_f$ of $Ba_{2-x}Ca_xMgTi_5O_{13}$ ceramics exhibits a monotonous change from negative values to positive

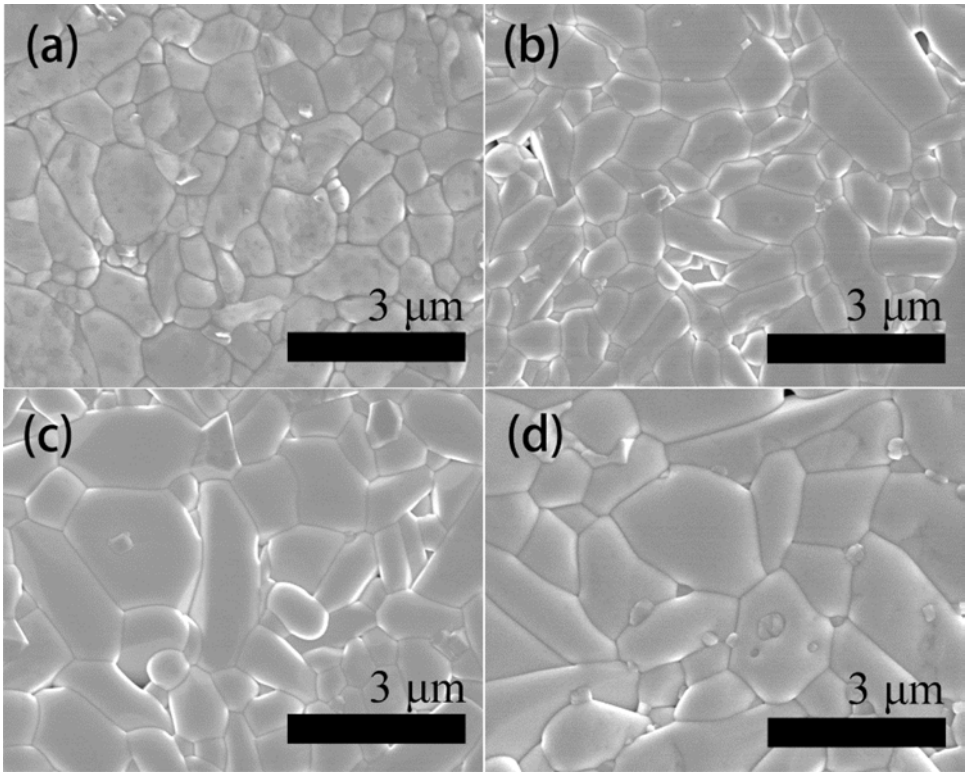


**Fig. 3.** SEM images on polished and thermally etched surfaces of $Ba_{2-x}Ca_xMgTi_5O_{13}$ ceramics sintered at optimum temperatures: (a) x = 0, (b) x = 0.05, (c) x = 0.15 and (d) x = 0.30.

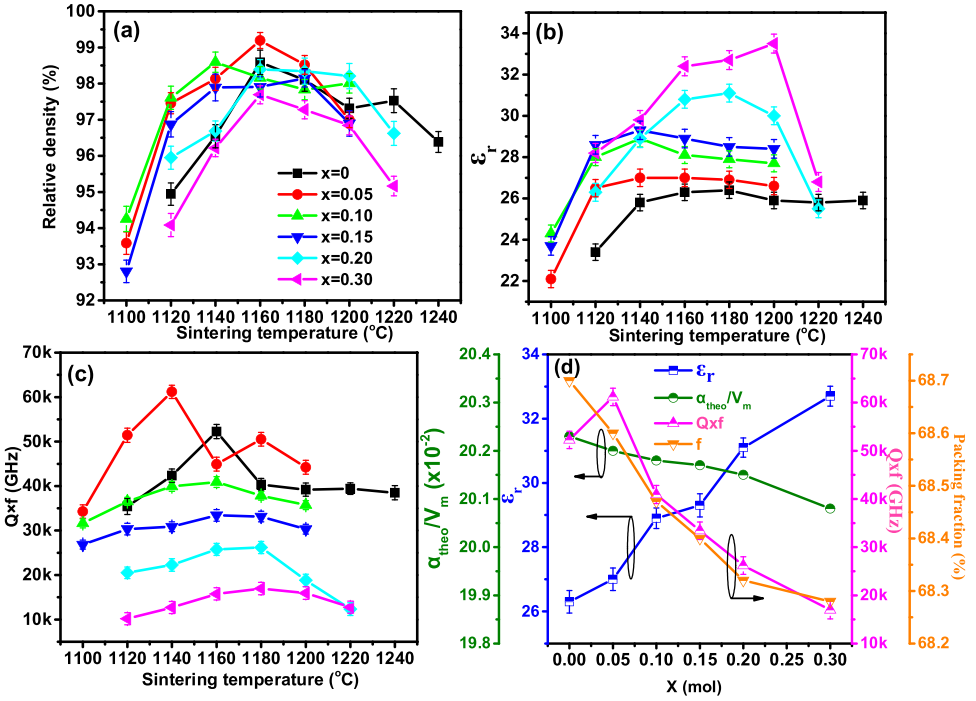


**Fig. 4.** (a) Relative density, (b) $\varepsilon_r$, (c) Qxf values of $Ba_{2-x}Ca_xMgTi_5O_{13}$ ceramics as a function of sintering temperature; and (d) the measured $\varepsilon_r$, Qxf, $\alpha_{theo}/V_m$ and packing fraction (f) of $Ba_{2-x}Ca_xMgTi_5O_{13}$ ceramics as a function of x.

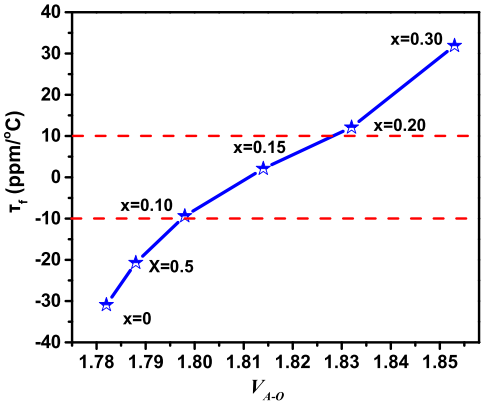


**Fig. 5.** The $\tau_f$ values against the A-site bond valence $V_{A-O}$ for $Ba_{2-x}Ca_xMgTi_5O_{13}$ ceramics as indicated.

values with increasing x. Near-zero $\tau_f$ values can be obtained approximately at x = 0.15. It is believed that the bond valence of the structure is one of the key factors affecting $\tau_f$ values of ceramics. The bond valence of ions ($V_i$) defined as the sum of all of the valences from a given atom i, as expressed by the following equations [20]:

$$V_i = \sum v_{ij} \tag{3}$$

$$v_{ij} = exp\left\{\frac{(R_{ij} - d_{ij})}{b}\right\} \tag{4}$$

where $v_{ij}$ is the bond valence between atoms i and *j*, $R_{ij}$ is the bond valence parameter, $d_{ij}$ is the length of a bond between atoms i and *j*, and b is commonly taken to be a universal constant equal to 0.37 Å. The bond valence parameters follow the values in a previous report [21]. As $Ba^{2+}$ in $Ba_2MgTi_5O_{13}$ was substituted by $Ca^{2+}$ in current work, an appropriate understanding of the coordination condition of $Ba^{2+}$ would be necessary. From the refinement results, the each bond length for $Ba^{2+}$ ions to oxygen ions, and the coordination condition of $Ba^{2+}$ ions can be obtained. Ba ions are surrounded by eight O ions and thus there exist four kinds of O ions, each of which possesses two equivalent O ions in connection with Ba ions. The details of the bond length and A-site bond valence are listed in Table 1. The variation of $\tau_f$ value and A-site valence in $Ba_{2-x}Ca_xMgTi_5O_{13}$ samples as a function of x is shown in Fig. 5. With increasing $Ca^{2+}$ content, the A-site bond valence gradually increases, thus contributing to the increase of $\tau_f$ values. As known, the A-site ionic substitution has been widely attempted owing to its role in tailoring undesirable $\tau_f$ values of the matrix by forming a solid solution. It was previously revealed that the substitution of Ni ions for Zn ions contributes to the decrease of the A-site bond valence and consequently the decrease of $\tau_f$ values in the monoclinic structured $(Zn_{1-x}Ni_x)_3Nb_2O_8$ system [22,23]. In current work, the substitution of smaller $Ca^{2+}$ for bigger $Ba^{2+}$ tends to increase the restoring force for recovering the tilting of polyhedron. As a result, $\tau_f$ value undergoes a considerable change from negative to positive values.

## 4. Conclusions

In this work, a new microwave dielectric ceramic $Ba_{2-x}Ca_xMgTi_5O_{13}$ was successfully synthesized by a conventional solid-state method. The phase composition, sintering behavior, microstructure and microwave dielectric properties were investigated as function of sintering temperature and the substitution content. The substitution of $Ca^{2+}$ for $Ba^{2+}$ provokes the formation of solid solutions in the experimental composition range. All the studied samples exhibit dense microstructures with a high relative density of < 96%. The $Ca^{2+}$ substitution induces the lattice distortion (reduced packing fraction) and uneven grain growth, contributing to decreased Qxf values, but increased $\varepsilon_r$ values although both the sample density and the ratio of the theoretical ionic polarizability to the molar volume ($\alpha_D/V_m$) vary very slightly. Moreover, a reduced A-site bond valence induced by $Ca^{2+}$ substitution leads to a desirable modification of $\tau_f$ from negative to positive values. In addition to relatively low sintering temperature and low cost of raw materials compared with some commercial medium-permittivity dielectrics such as $Ba(Mg,Ta,Sb)O_3$ and $(Sm,Nd)AlO_3$ perovskites, the x = 0.15 composition sintered at 1160 °C for 4 h exhibits good microwave dielectric properties of $\varepsilon_r$ = 29.3,Qxf = 30,870 GHz (at 6.5 GHz),

and $\tau_f = +2.1$ ppm/°C, showing large application potentials in future microwave devices.

## Acknowledgement

Financial support from the Natural Science Foundation of Anhui Province (1508085JGD04) is gratefully acknowledged.

## References

[1] R. Freer, F. Azough, Microstructural engineering of microwave dielectric ceramics, J. Eur. Ceram. Soc. 28 (2008) 1433–1441.
[2] T.A. Vanderah, Talking ceramics, Science 298 (2002) 1182–1184.
[3] I.M. Reaney, D. Iddles, Microwave dielectric ceramics for resonators and filters in mobile phone networks, J. Am. Ceram. Soc. 89 (2006) 2063–2072.
[4] S.G. Mhaisalker, D.W. Readey, S.A. Akbar, Microwave dielectric properties of doped $BaTi_4O_9$, J. Eur. Ceram. Soc. 74 (1991) 1894–1898.
[5] J.K. Plourde, D.F. Linn, H.M. O'Bryan, J. Thomson, $Ba_2Ti_9O_{20}$ as a microwave dielectric resonator, J. Am. Ceram. Soc. 58 (1975) 418–420.
[6] S.Q. Yu, B. Tang, S.R. Zhang, X.H. Zhou, Effect of Zn ratio on sintering behavior and microwave dielectric properties of BaO-ZnO-$TiO_2$ ceramics, J. Alloys. Compd. 505 (2010) 814–817.
[7] G.Q. Wang, S.H. Wu, H. Su, Microwave dielectric ceramics in the BaO-ZnO-$TiO_2$ system doped with $MnCO_3$ and $SnO_2$, Mater. Lett. 59 (2005) 2229–2231.
[8] J.P. Guha, D. Kolar, B. Volavsek, Preparation and characterization of new ternary compounds in the system BaO-$TiO_2$-$Al_2O_3$, J. Solid Chem. 16 (1976) 49–54.
[9] R. Ratheesh, H. Sreemoolanadlhan, S. Suma, M.T. Sebastian, K.A. Jose, P. Mohanan, New high permittivity and low loss ceramics in BaO-$TiO_2$-$Nb_2O_5$ composition, J. Mater. Sci. Mater. Electron. 9 (1998) 291–294.
[10] H. Yamada, T. Okawa, Y. Tohda, H. Ohsato, Microwave dielectric properties of $Ba_xLa_4Ti_{3+x}O_{12+3x}$ (x = 0.0-1.0) ceramics, J. Eur. Ceram. Soc. 26 (2006) 2059–2062.
[11] H. Ohsato, S. Nishigaki, T. Okuda, Superlattice and dielectric propertied of BaO-$R_2O_3$-$TiO_2$ (R = La, Nd, and Sm) microwave dielectric compounds, J. Appl. Phys. 31 (1992) 3136–3168.
[12] Y.P. Fu, C.W. Liu, C.H. Lin, C.K. Hsieh, Effect of $TiO_2$ ratio on BaO-$Nd_2O_3$-$TiO_2$ microwave ceramics, Ceram. Int. 31 (2005) 667–670.
[13] R.S. Roth, C.J. Rawn, C.G. Lindsay, W. Wong, Phase equilibria and crystal chemistry of the binary and ternary barium polytitanates and crystallography of the barium zinc polytitanates, J. Solid State Chem. 104 (1993) 99–118.
[14] A.G. Belous, O.V. Ovchar, M.K. Marjeta, M. Valant, The homogeneity range and the microwave dielectric properties of the $BaZn_2Ti_4O_{11}$ ceramics, J. Eur. Ceram. Soc. 26 (2006) 3733–3739.
[15] M.T. Sebastian, New low loss microwave dielectric ceramics in the BaO-$TiO_2$-$Nb_2O_5$/$Ta_2O_5$ system, J. Mater. Sci. Mater. Electron. 10 (1999) 475–478.
[16] X.L. Chen, H.F. Zhou, L. Fang, L.J. Liu, C.D. Li, R.L. Guo, H. Wang, Low-temperature sintering and compatibility with silver electrode of $Ba_4MgTi_{11}O_{27}$ microwave dielectric ceramic, Mater. Res. Bull. 45 (2010) 1509–1512.
[17] E.E. Havinga, The temperature dependence of dielectric constant, J. Phys. Chem. Solids 18 (1961) 253–255.
[18] R.D. Shannon, Dielectric polarizabilities of ions in oxides and fluorides, J. Appl. Phys. 73 (1993) 348–366.
[19] Y.C. Chen, Y.N. Wang, C.H. Hsu, Enhancement microwave dielectric properties of $Mg_2SnO_4$ ceramics by substituting $Mg^{2+}$ with $Ni^{2+}$, Mater. Chem. Phys. 133 (2012) 829–833.
[20] E.S. Kim, C.H. Jeon, P.G. Clem, Effects of structure on microwave dielectric properties of $ABO_4$ (A = Ni, Mg, Zn and B = Mo, W) ceramics, J. Am. Ceram. Soc. 95 (2012) 2934–2938.
[21] N.B. Brese, M. O'Keefe, Bond-valence parameters for solids, Acta Crystallogr. B 47 (2) (1991) 192–197.
[22] C.L. Huang, W.R. Yang, P.C. Yu, High-Q microwave dielectrics in low- temperature sintered $(Zn_{1-x}Ni_x)_3Nb_2O_8$ ceramics, J. Eur. Ceram. Soc. 34 (2014) 277–284.
[23] H.S. Park, K.H. Yoon, E.S. Kim, Effect of bond valence on microwave dielectric properties of complex perovskite ceramics, Mater. Chem. Phys. 79 (2003) 181–183.